Proceedings of ASME Turbo Expo 2011
GT2011
June 6-10, 2011, Vancouver, British Columbia, Canada

GT2011-45346

NOVEL DYNAMIC ROTOR AND BLADE DEFORMATION AND VIBRATION MONITORING TECHNIQUE

Thorsten Pfister
Technische Universität Dresden, Laboratory for Measurement and Testing Techniques
Helmholtzstrasse 18, 01062 Dresden, Germany
phone: +49 351 463-35303
e-mail: thorsten.pfister@tu-dresden.de

Philipp Günther
Technische Universität Dresden, Laboratory for Measurement and Testing Techniques
Helmholtzstrasse 18, 01062 Dresden, Germany
phone: +49 351 463-39809
e-mail: philipp.guenther@tu-dresden.de

Florian Dreier
Technische Universität Dresden, Laboratory for Measurement and Testing Techniques
Helmholtzstrasse 18, 01062 Dresden, Germany
phone: +49 351 463-42256
e-mail: florian.dreier@tu-dresden.de

Jürgen Czarske
Technische Universität Dresden, Laboratory for Measurement and Testing Techniques
Helmholtzstrasse 18, 01062 Dresden, Germany
phone: +49 351 463-34803
e-mail: juergen.czarske@tu-dresden.de

ABSTRACT

Monitoring rotor deformations and vibrations dynamically is an important task for improving both the safety and the lifetime as well as the energy efficiency of motors and turbo machines. However, due to the high rotor speed encountered in particular at turbo machines, this requires concurrently high measurement rate and high accuracy, which is hardly possible to achieve with currently available measurement techniques. To solve this problem, in this paper, we present a novel non-incremental interferometric optical sensor that measures simultaneously the in-plane velocity and the out-of-plane position of laterally moving objects with micrometer precision and concurrently with microsecond temporal resolution. It will be shown that this sensor exhibits the outstanding feature that its measurement uncertainty is generally independent of the object velocity, which enables precise deformation and vibration measurements also at high rotor speed. Moreover, this sensor does not require an in situ calibration and it allows a direct measurement of blade velocity variations in contrast to BTT systems. For application under harsh environmental conditions such as high temperatures, a robust and miniaturized fiber-optic sensor setup was developed. To demonstrate the capability of this sensor, measurements of tip clearance changes and rotor blade vibrations at varying operating conditions of a transonic centrifugal compressor test rig at blade tip velocities up to 600 m/s are presented amongst others.

1 INTRODUCTION

In order to improve safety, lifetime and energy efficiency of turbo machines, in particular the dynamic behavior of the rotor has to be analyzed and optimized. Thus, rotor unbalances, dynamic deformations and blade vibrations have to be monitored during operation for optimizing the rotor design and to validate numerical models [1]. In particular, this holds for the development of modern aircraft engines employing extremely thin rotor blades or so called bliscs (blade-discs), which are even more susceptible to vibrations [2]. Furthermore, the blade tip clearance, which changes due to varying temperature and pressure conditions inside the machine, has to be minimized for enhancing efficiency. Therefore, an accurate and online determination of the tip clearance is required for implementing optimized automatic clearance control systems and to prevent fatal damage by blade rubbing [3,4]. However, these are big challenges for metrology, since contactless and non-incremental measurement techniques are required offering both micrometer accuracy and microsecond temporal resolution.

For tip clearance measurements, usually capacitive, inductive or eddy current probes are employed because they are robust and low cost [3-6]. However, these sensors are susceptible to electromagnetic interferences and they require an application dependent and time-consuming calibration since their measurement results strongly depend on the material and geometry of rotor and casing, respectively. In addition, they are also strongly influenced by the dielectric properties of the air in the gap between rotor and stator, which are changing with varying temperature and pressure inside the machine. Thus, these electrical tip clearance probes offer only a moderate accuracy of around (50…100) µm in practice, which is not sufficient for active clearance control systems that are currently under way [3,4,6]. In addition, capacitive as well as inductive and eddy current probes fail at modern non-metallic rotors out of ceramics or fiber-reinforced composites [7].

Optical measurement techniques overcome these drawbacks and offer higher accuracy. However, incremental sensors such as Michelson interferometers or laser scanning vibrometers are not applicable, because their measurement results become ambiguous if distance jumps of more than half the laser wavelength occur, e.g. at rough surfaces or from one rotor blade to the next. Furthermore, the measurement rate of most optical techniques is fundamentally limited either by the speed of mechanical scanning (time domain OCT, focus sensing) [8] or by the detector frame rate and minimum exposure time (triangulation, chromatic confocal techniques, frequency domain OCT) [9,10]. Furthermore, at rough surfaces, coherent speckle noise and shading are also problematic especially at triangulation [10]. Time-of-flight sensors [11] are limited due to the finite time resolution of the signal processing. Therefore, conventional optical sensors are not suitable for precise and highly dynamic measurements at high-speed rotors.

Concerning rotor deformation and vibration monitoring, strain gauges are commonly used [12]. However, their durability and application at the rotor and the signal transmission from the rotating system involves great effort, and major difficulties occur particularly at high rotor speed. Also scanning laser Doppler vibrometers [13] are not applicable for dynamic measurements inside turbo machines because of the limited optical access. Blade tip timing (BTT) systems used instead rely on delicate edge detection schemes and provide only an indirect measurement of blade velocity variations [5,12].

To overcome these problems of existing measurement techniques, we developed a novel non-incremental laser Doppler distance sensor (LDDS) [14-16], which is able to measure not only the in-plane velocity but, unlike conventional laser Doppler velocimeters, also the out-of-plane position of a moving solid surface non-incrementally and with micrometer precision. Thus, the shape of rotating objects can be measured absolutely and with a single sensor only [14]. The unique feature of this sensor is that its position uncertainty is generally independent of the object velocity in contrast to conventional distance sensors [15,17], which enables precise deformation and vibration measurements with high temporal resolution, i.e. also at high rotor speed [15-17]. Furthermore, this sensor does not require a laborious in situ calibration and it allows measuring tip clearance as well as radial and lateral blade vibrations simultaneously. Moreover, a direct measurement of blade velocity variations is possible in contrast to BTT systems.

In the following sections, the functional principle and the unique measuring properties of the LDDS are described in detail. In addition, a modular fiber-optic sensor setup featuring a robust and all passive measurement head is presented that is suitable for application under harsh environmental conditions occurring at turbo machines, such as high temperatures. To demonstrate the capability of this sensor, measurement results of dynamic rotor deformations and wobbling motions as well as measurements of turbo machine tip clearance changes and rotor blade vibrations under operating conditions at up to 50,000 rpm rotor speed corresponding to 600 m/s blade tip velocity are presented. Finally the most important results are summarized.

2 THE LASER DOPPLER DISTANCE SENSOR (LDDS)

2.1 Functional Principle

The LDDS is based on laser Doppler velocimetry (LDV) which is a well-established technique for measuring velocities of point-wise scattering particles in fluid flows and also of moved solids [18]. It evaluates the scattered light from measurement objects passing a measurement volume, which is formed by interference fringes in the intersection volume of two coherent laser beams. Taking into account the spacing d of the interference fringes, the velocity v of the measurement object is calculated by means of $v = f\,d$, with f denoting the measured Doppler frequency. However, due to the wave front curvature of Gaussian laser beams, the fringe spacing d is not constant but varies along the axial position z. This limits the achievable velocity measurement accuracy of conventional LDV sensors fundamentally since the object position z is not known.

The basic idea of the LDDS is to enhances this parasitic position dependency of the fringe spacing $d(z)$ significantly and to utilize it for determining the axial position z of the measurement object in addition to its tangential velocity v [14-16]. For this purpose, two superposed fan-shaped interference fringe systems with contrary fringe spacing gradients are generated inside the same measurement volume using wavelength division multiplexing (see Fig. 1). The fringe spacings $d_{1,2}(z)$ are monotonously increasing and decreasing functions with respect to the axial position z, i.e. with the distance. A wavelength-sensitive detection of the two resulting Doppler frequencies $f_{1,2}$ yields the quotient function [14-16]

$$q(z) = \frac{f_2(v,z)}{f_1(v,z)} = \frac{v/d_2(z)}{v/d_1(z)} = \frac{d_1(z)}{d_2(z)} \;, \qquad (1)$$

which is also a monotonous function that does no longer depend on the velocity v. Therefore, this quotient $q(z)$ can be used to determine the axial position z of the measurement object inside the measurement volume non-incrementally and independently of its velocity v. With the known position z, the actual fringe spacings d_1 and d_2 at the position of the measurement object can be identified via the calibrated fringe spacing curves $d_{1,2}(z)$. As a result, the velocity v can be calculated precisely according to

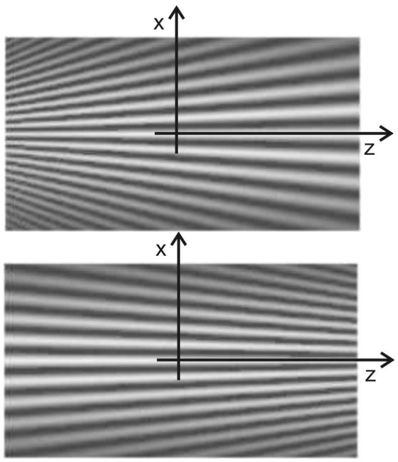

FIGURE 1. Two interference fringe systems with monotonously increasing (top) and decreasing (bottom) fringe spacing in axial direction *z* are shown, which are superposed in the same location in practice.

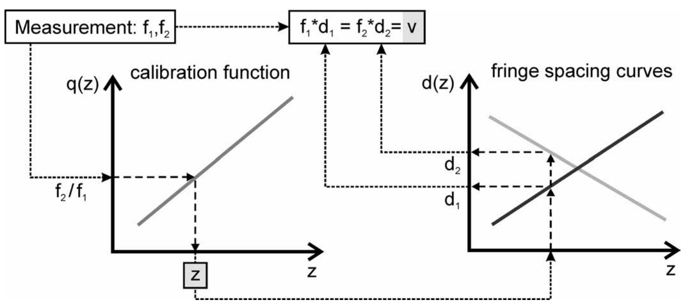

FIGURE 2. Functional principle of the laser Doppler distance sensor (LDDS).

$v = f_1\, d_1 = f_2\, d_2$. Thus, axial position z and tangential velocity v can be determined simultaneously and independently, see summary of the functional principle in Fig. 2.

2.2 Modular and Fiber-Optic Sensor Setup

For enabling measurements at turbo machines under operating conditions (high temperatures, vibrations), a modular and robust setup of the LDDS was realized consisting of three units: a light source unit, a robust and all-passive measurement head, and a detection unit, which were connected to each other via two 25 m long fiber patch cables (see Fig. 3) [15-17].

The light source unit contained two pigtailed single transverse mode laser diodes (λ_1 = 658 nm and λ_2 = 830 nm wavelength) combined by means of a 2x1 fused fiber coupler to one single mode fiber. The fiber optic measurement head for generating the two fan-shaped interference fringe systems was all passive to avoid electrical disturbances and it was equipped with radiator coils for water cooling making it immune against temperature influences. In order to obtain a compact and robust sensor head with a minimum number of adjustment elements, a special design using a diffractive optical element (DOE) was employed [19] (Fig. 3). The high dispersion of the diffractive lens effected an axial separation of the beam waists of the two different wavelengths of several millimeters at the beam splitting transmission grating. By contrast, the subsequent Kepler telescope for imaging the +1st and -1st diffraction orders of the grating to the measurement volume exhibited very low dispersion. Thus, two fan-shaped interference fringe systems with contrary fringe spacing gradients were generated at the same location defining the measurement volume. The outer dimensions of the measurement head were 200 x 82 x 54 mm^3. The bichromatic scattered light from the measurement object

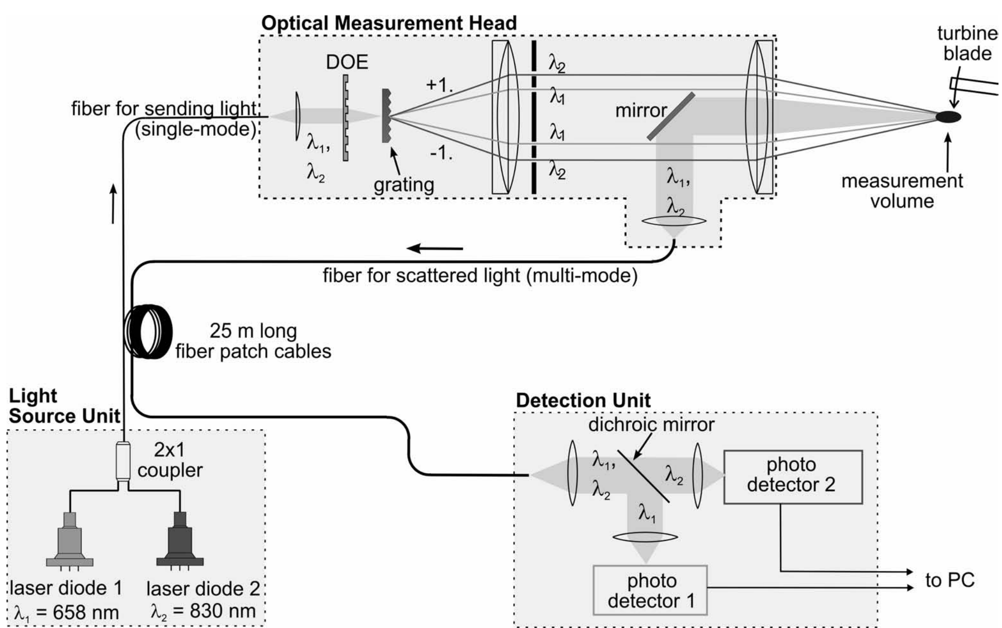

FIGURE 3. Modular and fiber-optic setup of the LDDS [16].

was detected in backward direction and coupled into a multimode fiber by a mirror and a single lens (see Fig. 3).

The detection unit split the received scattered light from the measurement object into the two different wavelengths by a dichroic mirror and focused it onto two high bandwidth photo detectors. The detector signals were fed via a 14 Bit A/D converter card into a standard PC for further processing.

2.3 Measuring Properties

The minimally attainable position standard uncertainty σ_z of the LDDS can be investigated by using the law of error propagation. Around the center of the measurement volume it can be approximated by [14]

$$\sigma_z \approx \sqrt{2}\left|\frac{\partial q(z)}{\partial z}\right|^{-1} \frac{\sigma_f}{f} \quad . \tag{2}$$

Due to this equation, the position resolution only depends on the slope of the quotient function dq/dz and on the relative uncertainty of the frequency measurement $\sigma_f\,/\,f$. Inserting the Cramer-Rao lower bound (CRLB) for the frequency measuring error of noisy single-tone signals and the relation for the Doppler frequency $f = v/d$, equation (2) can be rewritten as [17]

$$\sigma_z \approx \sqrt{2}\left|\frac{\partial q(z)}{\partial z}\right|^{-1} \frac{k \cdot d}{\Delta x \cdot \sqrt{SNR \cdot N}} \quad , \tag{3}$$

with k denoting a constant term. Consequently, besides the steepness of the quotient function, the minimum position uncertainty σ_z depends on the mean actual fringe spacing d, on the averaging length on the object surface Δx, on the signal-to-noise ratio SNR of the measured signals and on the number N of recorded samples per signal. However, the velocity v cancels out since the position measurement is attributed to a velocity measurement. Thus, the position uncertainty of the LDDS is generally independent of the object velocity in contrast to conventional distance measurement techniques. This unique feature of the LDDS can be proven both theoretically (cp. equation (3)) and experimentally (see Fig. 4). Therefore, position measurements with micrometer precision can be carried out even at extremely fast moving objects, such as turbo machine rotors.

Furthermore, the velocity measurement uncertainty of the LDDS is not degenerated by fringe spacing variations inside the measurement volume unlike conventional LDV, since the actual fringe spacings d_1 and d_2 can be identified via the known object position z (see above). Thus the LDDS enables more precise velocity measurements than conventional LDV sensors [14,15].

In addition, the LDDS is not strongly influenced by coherent speckle noise and shading effects are significantly reduced compared to triangulation [14]. Moreover, high measurement rates are possible since this sensor does not contain any mechanically moved parts and because high

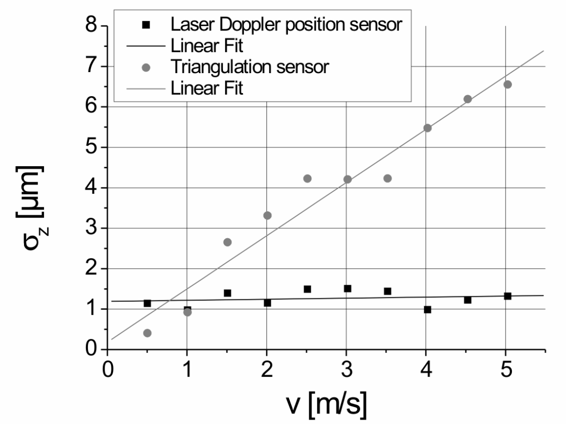

FIGURE 4. Experimentally obtained standard position uncertainties σ_z are shown, which were obtained using a rotating brass toothed wheel with 40 mm radius and 2 mm tooth width [17]. For the commercial triangulation sensor, the position uncertainty increases steadily with increasing circumferential speed v, whereas σ_z remains approximately constant for the LDDS at a value slightly above 1 µm.

bandwidth photo detectors are employed (cp. section 2.2). Consequently, the LDDS overcomes the disadvantages of conventional distance sensors and offers concurrently high temporal resolution and high position resolution in the micron range. Thus, this sensor is predestined for precise and real-time deformation and vibration monitoring of high-speed rotors, e.g. of turbo machines.

Moreover, the calibration data of the LDDS are independent of the material and the geometry of the rotor and the blades, respectively. Thus, a laborious in-situ calibration for each measuring task, i.e. at each measuring point is not necessary unlike e.g. capacitive probes. In addition, measurements are also possible at non-metallic rotors. Besides, a direct measurement of the actual blade tip velocities and of their variations is possible in contrast to BTT systems, which are only able to measure average velocities within a certain period. All in all, the LDDS allows measuring tip clearance as well as radial and lateral blade vibrations simultaneously.

3 EXPERIMENTAL RESULTS

3.1 Measurements of Dynamic Rotor Expansion and Wobbling

For efficiency and safety reasons, it is important to investigate the elastic and plastic deformation behavior of high speed rotors in dependence of the rotational speed. Particularly in composite materials such as fiber-reinforced plastics, experimental tests are necessary since these materials cannot be simulated reliably due to their anisotropic properties. Of particular interest is the radial expansion due to centrifugal forces that can cause a failure of the device at high speed.

Such experiments can be carried out at the vacuum high-speed rotor test rig of the institute of lightweight construction and polymer technology (ILK) at the Technische Universität Dresden. The test rig consists of a metallic container integrated in the basement, a swivel-mounted top cover with lifting gear and changeable planetary drive and a synchronous motor which is attached to the planetary drive by a belt. The test objects are only unilaterally mounted to the top cover of the test rig (see Fig. 5, bottom) which provokes additional wobbling motions. Depending on the mass of the test object, the test rig can be operated at rotation speeds of up to 250,000 rpm.

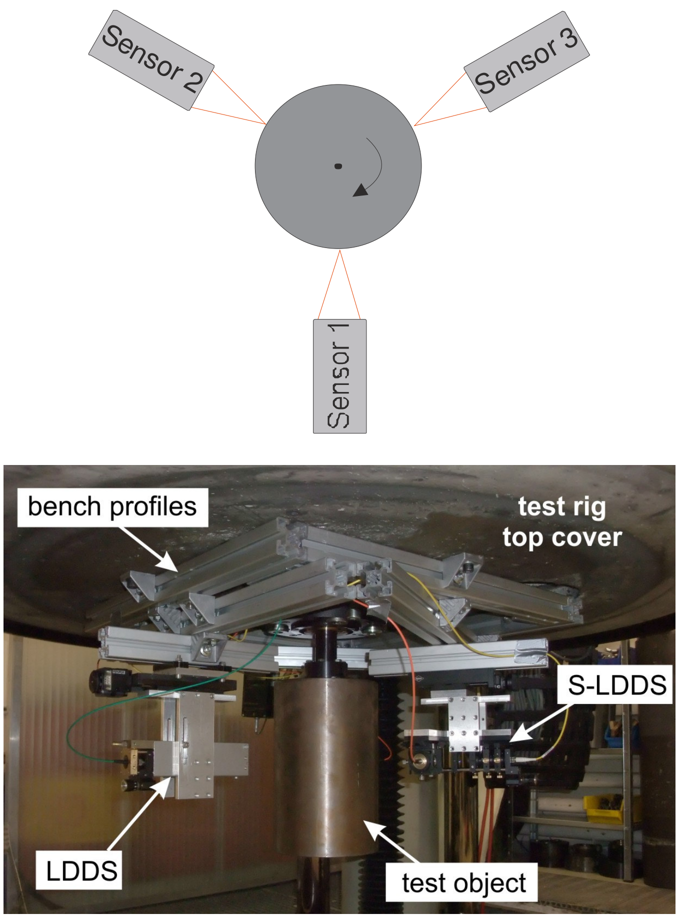

FIGURE 5. Top: schematic of the configuration of the 3-point measurement system. Bottom: picture of the test object (steel cylinder) and of the LDDS sensors attached to the top cover of the test rig.

To investigate the test objects in this test rig, the dynamic rotor deformations and the wobbling motion of the object have to be measured simultaneously. Thus, a 3-point LDDS measurement system is necessary as shown in Fig. 5 [20]. The three sensors are arranged at the same object height but at different angular positions along the object circumference with offsets of 120° against each other. Furthermore, all three sensors are directed to the object rotation axis which coincides with its center of mass assuming a cylindrical object shape. The measured position values of the three sensors are corresponding to three points in a plane, which are unambiguously defining a circle representing the size and the position of the cylindrical test object [20]. Assuming that the mean object radius $\overline{R}$ is much larger than the radial expansions ΔR caused by speed or temperature as well as much larger than the amplitude of occurring wobbling motions, the radial alignment of the sensors with respect to the object rotation axis will be always maintained in good approximation.

Here, as a test object, a cylindrical rotor out of steel was used exhibiting a radius of R = 95 mm, a height of 300 mm and a mass of about 60 kg. For safety reasons, the rotation speed was restricted at this experiment to a maximum of 12,000 rpm corresponding to a maximum surface velocity of around 120 m/s. All measurements were accomplished both at normal atmospheric air pressure of 1 bar and at low vacuum pressure of 5 mbar (= $5 \cdot 10^{-3}$ bar).

Figure 6 (top) depicts the measured variation in time of the center of mass in x_c- and y_c-directions for a rotational speed of 2000 rpm as well as a two-dimensional map for the corresponding wobbling motion (Fig. 6, bottom). For better visibility of the wobbling, regression curves were fit to the raw data. The peak-to-peak amplitude of the wobbling in x_c- as well as in y_c-direction amounts to about 200 µm at maximum. Furthermore, the amplitudes are time-variant pointing out that the wobbling is not stationary, which is clearly visible in the two-dimensional map shown on bottom of Fig. 6.

For a quantitative analysis of the dependency of the wobbling magnitude against the rotation speed, the standard deviations of the variations of the center of mass were calculated according to

$$\sigma_{center\,of\,mass} = \sqrt{\sigma_{x_c}{}^2 + \sigma_{y_c}{}^2} \ . \tag{4}$$

As a result, it can be seen in Fig. 7 that the wobbling amplitude is maximal at a rotational speed of 2000 rpm representing a resonance point and that it is strongly decreasing towards higher rotor speed. Furthermore, there are no significant differences between the measurements at normal atmospheric air pressure and under low vacuum.

In addition, the radial enlargement of the test rotor has been evaluated in dependence of the rotation speed. According to theory, the radial rotor enlargement is directly proportional to the square of the rotation speed $f_{rot}{}^2$. The obtained measurement results agree very well with this theory as indicated by the quadratic regression curve included in Fig. 8. Unfortunately, it was not possible to include a corresponding simulation curve since the object material parameters and the ambient conditions at the test rig were not known in detail. However, rough estimates of the theoretically expected radial enlargement were in the same range as the measurement results of Fig. 8.

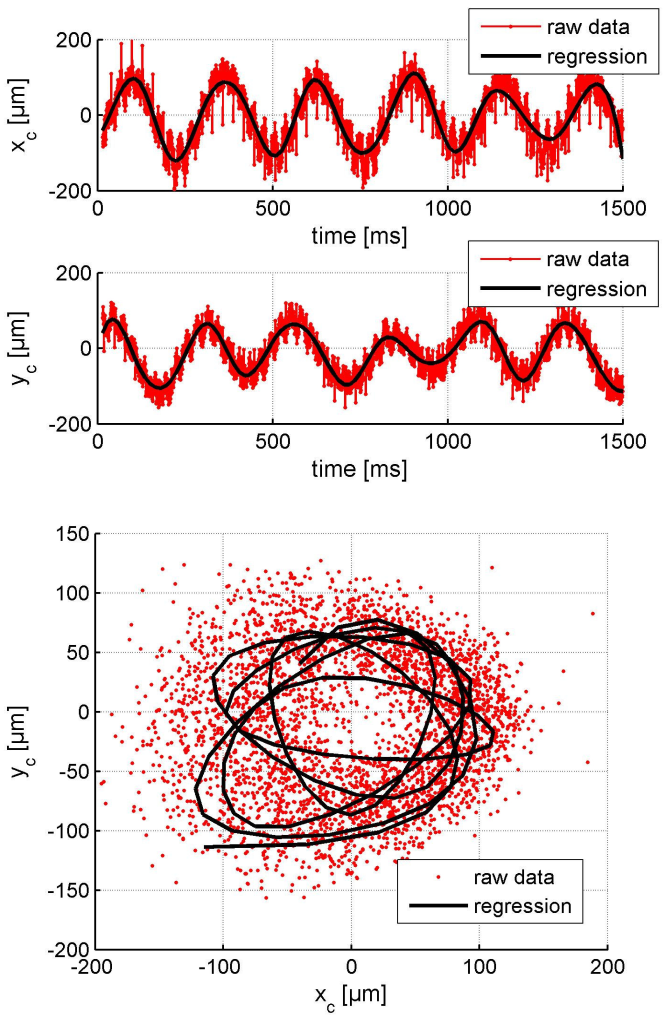

FIGURE 6. Measured dynamic displacement of the center of rotation, i.e. the center of mass, $(x_c,y_c)^T$ of a cylindrical steel rotor over time (top) and corresponding two-dimensional map of the wobbling motion (bottom). The solid black lines represent regression curves for visualizing the wobbling motion [20].

Thus, these experimental results demonstrate that wobbling motions as well as dynamic deformations (radial enlargement) of rough solid rotors can be measured simultaneously and independently using a multi-point LDDS measurement system. The obtained accuracies are in the range of some micrometers as indicated by the error bars in Fig. 8. Due to the velocity independent measurement uncertainty of the LDDS, these measurements can be carried out also at high rotor speed. Furthermore, the presented results show that the LDDS can be applied under varying pressure conditions including vacuum.

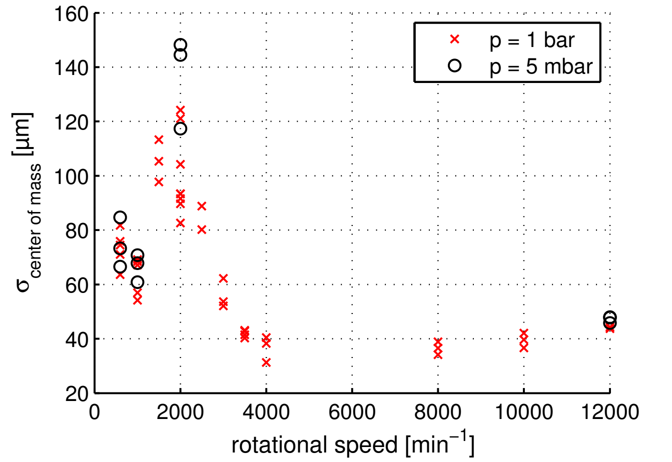

FIGURE 7. Measured wobbling magnitudes represented by the standard deviations of the center of mass in dependence on the rotational speed.

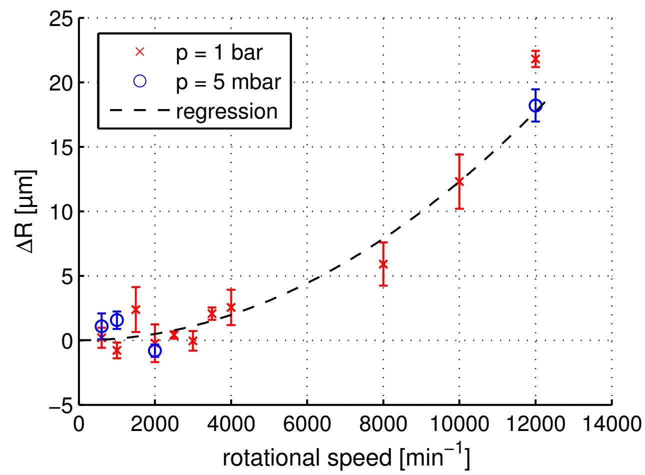

FIGURE 8. Measured radial enlargements of the test rotor as a function of its rotational speed in comparison with a quadratic regression curve [20].

3.2 Tip Clearance and Rotor Vibration Measurements at a Transonic Centrifugal Compressor

In order to demonstrate the capability of the LDDS in particular concerning turbo machine monitoring, it has been applied at a transonic centrifugal compressor test rig of the German Aerospace Center (DLR) Köln, Institute for Propulsion Technology. The fiber-coupled optical measurement head (cp. Fig. 3) was attached to the compressor casing and the beams were directed onto the rotor blades through a small glass window, which was mounted flush with the inner contour of the casing (see Fig. 9). The light source unit, the detection unit and the PC were set up in the control room adjacent to the test rig. In addition, the compressor casing was equipped with three capacitive probes equally distributed on the perimeter (see Fig. 9), which were used as a reference.

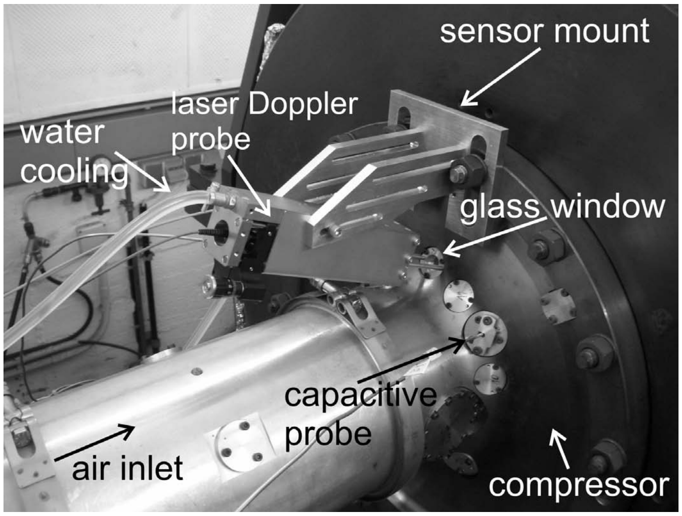

FIGURE 9. Compressor section of the test rig at the German Aerospace Centre (DLR) in Köln with the mounted laser Doppler probe (LDDS).

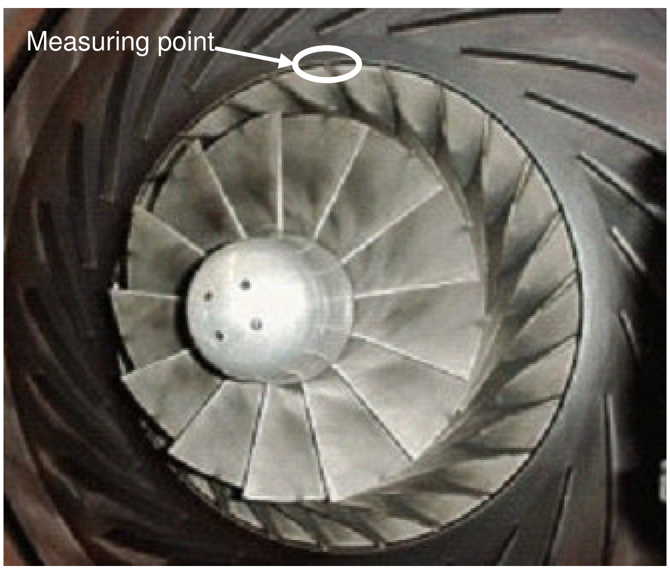

FIGURE 10. View to the compressor rotor when the casing is removed. The measuring point was located at the outermost radial part of the rotor blades

The compressor rotor had a radius of 112 mm and was equipped with 26 blades of 1.7 mm thickness at the tip. The measuring point was located at the outermost radial part of the rotor blades, which is the exit for the compressed air (see Fig. 10). The blade tip roughness was sufficient to generate Doppler modulated scattered light signals; no special treatment of the tips was necessary. Furthermore, the LDDS was calibrated only in the lab prior to the measurements; at the test rig, no specific calibration was required. A maximum rotational speed of 50,000 rpm (833 Hz) could be achieved, which corresponds to a blade frequency of 21.667 kHz and a circumferential speed of 586 m/s at the measurement position. Despite the high blade frequency and the resulting short transit time down to only 2.9 µs, the individual rotor blades could be resolved due to the high temporal resolution of the LDDS. During operation, the compressor temperature rose up to 280°C. The water cooling of the sensor head worked effectively keeping its temperature stable at about 18°C. Also no disturbing contamination of the glass window could be observed.

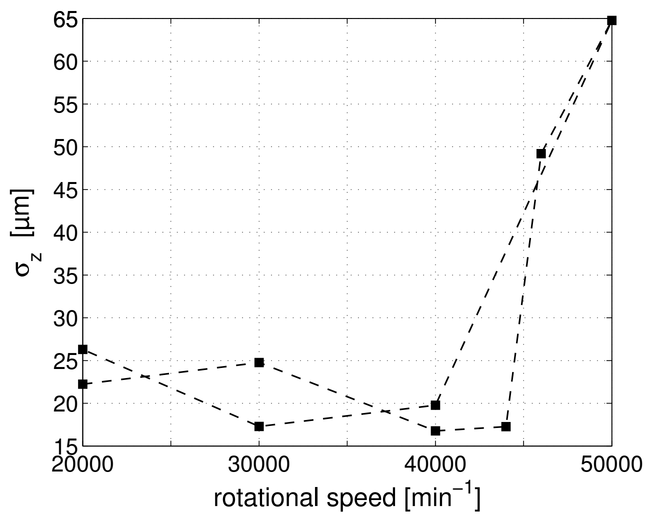

FIGURE 11. Standard position uncertainty σ_z for one single rotor blade in dependency of the rotor speed [17].

For determining the measurement uncertainty of the LDDS, the standard deviations σ_z of the measured blade tip positions over 80 consecutive revolutions were calculated for each rotor blade during power up and shut down of the compressor. The result is shown in Fig. 11 for one single rotor blade. Below 45,000 rpm, the standard deviations are between 17 µm and 26 µm resulting in an average standard position uncertainty of only 20.6 µm including unknown systematic errors [17]. This is much better than the uncertainty of conventional capacitive probes of about 50 µm [6]. Above 45,000 rpm, there is a strong increase in σ_z. This increase turned out to be caused by vibrations of the compressor rotor with a frequency of one third of the rotary frequency f_{rot}, which are visible in the time series and as well as in the corresponding spectra of the measured blade positions depicted in Fig. 12. The position uncertainty of the sensor itself is independent of the rotor speed (see section 2.3). Consequently, the LDDS is capable of detecting rotor and blade vibrations due to its high temporal resolution.

Further measurements were performed at a constant maximum rotational speed of 50,000 rpm. The tip clearance was successively increased by throttling the compressor. An appropriate low pass filter was applied to the measured blade position signals for removing the oscillations at 1/3 of the rotary

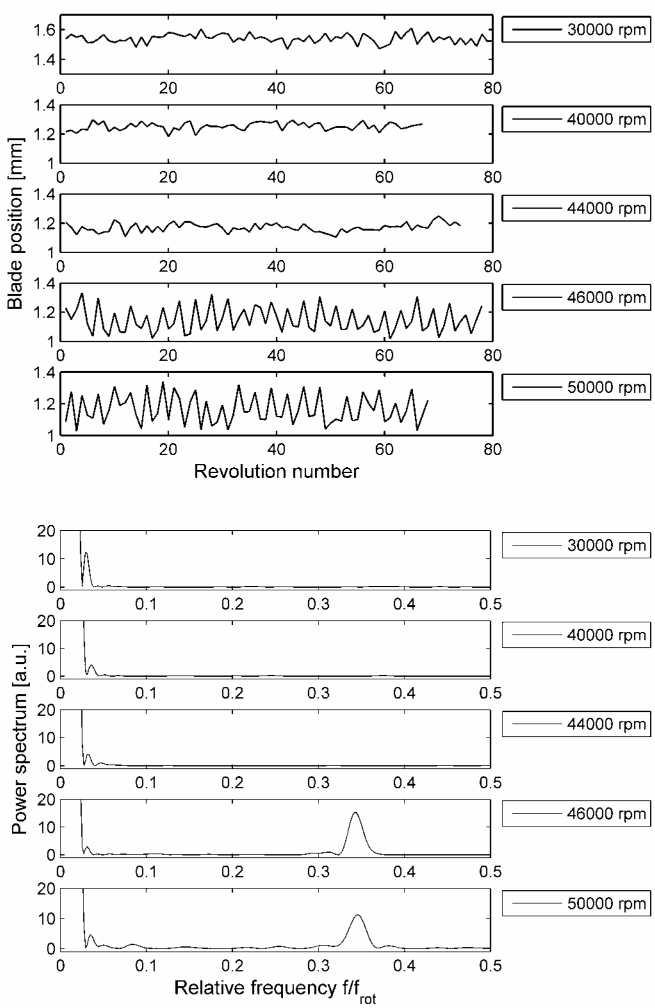

FIGURE 12. Position time series (top) and corresponding Fourier spectra (bottom) measured with the LDDS on a single rotor blade for five different rotational frequencies between 30,000 rpm and 50,000 rpm [17].

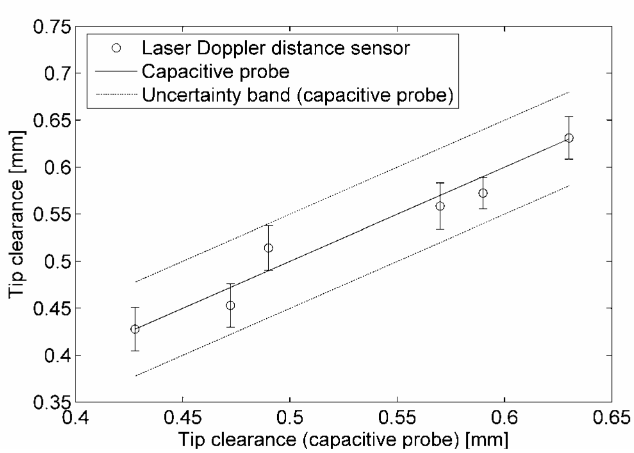

FIGURE 13. Blade tip clearance changes at varying mass flux of the centrifugal compressor test rig measured at 50,000 rpm with the LDDS in comparison with a capacitive reference probe [17].

frequency, which are physically generated by axial rotor vibrations and which do not represent a measurement error of the LDDS [17]. The measurement results for the LDDS averaged over 65 consecutive rotor revolutions are depicted in Fig. 13 in dependency of the tip clearances measured with the capacitive reference probes. The error bars mark the standard deviations for the LDDS. For comparison, the solid curve indicates the tip clearance measured with the capacitive probes including an uncertainty interval of ±50 µm. An excellent agreement occurs between the data of both sensors. Moreover, the achieved average position uncertainty of the LDDS of about 22 µm is significantly better than that of the conventional capacitive tip-clearance probes.

4 SUMMARY

A novel non-incremental laser Doppler distance sensor (LDDS) was developed and applied to monitoring dynamic deformations, such as radial expansion and resulting tip clearance changes, wobbling motions and vibrations of high speed rotors, which is a crucial task in order to improve the safety and the lifetime as well as the energy efficiency of motors and turbo machines.

The LDDS measures simultaneously the in-plane velocity and the out-of-plane position of laterally moving rough solid objects enabling the concurrent determination of both blade tip clearance changes and radial as well as lateral blade tip vibrations. It was shown theoretically as well as experimentally that a high temporal resolution (high measurement rate) in the microsecond range and a high position resolution in the micrometer range can be achieved simultaneously since the measurement uncertainty of the LDDS is generally independent of the object velocity (i.e. rotational frequency) in contrast to conventional distance sensors. This outstanding feature allows precise and dynamic deformation and vibration measurements even at very high rotor speed. Moreover, the LDDS does not require a laborious in situ calibration for each measuring task, unlike e.g. capacitive probes, and it allows a direct measurement of blade velocity variations in contrast to BTT systems. In order to cope with the harsh environmental conditions such as high temperatures occurring at turbo machines, a modular, robust and all-passive fiber-optic sensor setup was realized.

To evidence the capability of the LDDS, measurement results of dynamic rotor deformations (radial expansion) and wobbling motions as well as measurements of turbo machine tip clearance changes and rotor blade vibrations under operating conditions at up to 50,000 rpm rotor speed corresponding to 600 m/s blade tip velocity were presented. The experimental results demonstrate that the LDDS is able to achieve measurement accuracies in the micrometer range also at high rotor speed and under demanding environmental conditions, such as high temperatures and pressure variations from several bars down to low vacuum. In particular concerning tip clearance measurements, the obtained standard uncertainty of about

20 µm is significantly superior to the uncertainty of conventional capacitive probes. Moreover, the available measuring time amounted to only 2.9 µs at these tip clearance measurements, which shows the high temporal resolution of the LDDS.

Consequently, the novel LDDS opens up new perspectives for monitoring the dynamic behavior of high speed rotors, which is essential for improving both lifetime and energy efficiency of turbo machines, such as aircraft engines.

ACKNOWLEDGMENTS

The authors thank R. Schodl, H. Krain, M. Beversdorff, H. Fischer and J. Schlappa (DLR, Cologne, Germany) for their support at the compressor test rig and for fruitful discussions. Furthermore, we thank W. Hufenbach, A. Langkamp and T. Haupt (ILK, TU Dresden) for providing the vacuum high-speed rotor test rig and for supporting our measurements. Also the financial support from the Deutsche Forschungsgemeinschaft (DFG) (funding code: Cz55/19-1) is greatly acknowledged.

NOMENCLATURE

d	interference fringe spacing
f	Doppler frequency
f_{rot}	rotational speed
k	constant term
q	quotient of the two Doppler frequencies
v	velocity
x	direction of object movement perpendicular to z-axis
Δx	lateral averaging length on the object surface
x_c	x-coordinate of center of mass
y_c	y-coordinate of center of mass
z	axial position / distance
λ	laser wavelength
$\sigma_{center\ of\ mass}$	standard deviation of the radial movement of the center of mass
σ_f	standard uncertainty of frequency measurement
σ_z	standard uncertainty of position measurement
N	number of samples
R	radius
$\overline{R}$	mean object radius
ΔR	radial expansion
SNR	signal-to-noise ratio

REFERENCES

[1] Schweizer, B., and Sievert, M., 2009, „Nonlinear Oscillations of Automotive Turbocharger Turbines," Journal of Sound and Vibration, 321, pp. 955–975.

[2] Klauke, T., Kuhhorn, A., Beirow, B., et al., 2008, "Blade Vibration Phenomena of HPC Bliscs Considering Manufacturing Effects and Strain Gauge Application," Proceedings of 53rd ASME Turbo Expo 2008, ASME, New York, Vol. 5, Part A, pp. 403-413.

[3] Fabian, T., Prinz, F.B., and Brasseur, G., 2005, "Capacitive Sensor for Active Tip Clearance Control in a Palm-Sized Gas Turbine Generator," IEEE Trans. Instrum. Meas., 54, pp. 1133–1143.

[4] Lattime, S.B., and Steinetz, B.M., 2004, "High-Pressure-Turbine Clearance Control Systems: Current Practices and Future Directions," Journal of Propulsion and Power, 20, pp. 302-311.

[5] Lawson, C.P., and Ivey, P.C., 2005, "Turbomachinery Blade Vibration Amplitude Measurement through Tip Timing with Capacitance Tip Clearance Probes," Sensor and Actuators A, 118, pp. 14-24.

[6] Sheard, A.G., O´Donnell S.G., and Stringfellow, J.F., 1999, "High Temperature Proximity Measurement in Aero and Industrial Turbomachinery," Journal of Engineering Gas Turbines and Power, 121, pp. 167-173.

[7] Chakravarty, U.K., 2010, "SectionBuilder: An Innovative Finite Element Tool for Analysis and Design of Composite Rotor Blade Cross-Sections," Composite Structures, 92, pp. 284-294.

[8] Kempe, A., Schlamp S., and Rösgen, T., 2003, "Low-Coherence Interferometric Tip-Clearance Probe," Optics Letters, 28, pp. 1323–1325.

[9] Matsuda, Y., and Tagashira, T., 2001, "Optical Blade-Tip Clearance Sensor for Non-Metal Gas Turbine Blade," J. Gas Turbine Soc. Japan (GTSJ), 29, pp. 479–484.

[10] Dorsch, R.G., Häusler, G., and Herrmann, J.M., 1994, "Laser Triangulation: Fundamental Uncertainty in Distance Measurement," Applied Optics, 33, pp. 1306–1314.

[11] Dhadwal, H.S., and Kurkov, A.P., 1999, "Dual-Laser Probe Measurement of Blade-Tip Clearance," J. Turbomach., 121, pp. 481–485.

[12] Knappett, D., and Garcia, J., 2008, "Blade Tip Timing and Strain Gauge Correlation on Compressor Blades," Proc. IMechE Part G: J. Aerospace Engineering, 222, pp. 497-506.

[13] Oberholster, A.J., and Heyns, P.S., 2009, "Online Condition Monitoring of Axial-Flow Turbomachinery Blades using Rotor-Axial Eulerian Laser Doppler Vibrometry," Mechanical Systems and Signal Processing, 23, pp. 1634–1643.

[14] Pfister, T., Büttner, L., and Czarske, J., 2005, "Laser Doppler Profile Sensor with Sub-Micrometre Position Resolution for Velocity and Absolute Radius Measurements of Rotating Objects," Meas. Sci. Technol., 16, pp. 627-641.

[15] Pfister, T., 2008, "Untersuchung neuartiger Laser-Doppler-Verfahren zur Positions- und Formvermessung bewegter Festkörperoberflächen," Ph.D. Thesis, Technische Universität Dresden, Shaker, Aachen.

[16] Büttner, L., Pfister, T., and Czarske, J., 2006, "Fiber-Optic Laser Doppler Turbine Tip Clearance Probe," Optics Letters, 31, pp. 1217-1219.

[17] Pfister, T., Büttner, L., Czarske, J., Krain, H., and Schodl, R., 2006, “Turbo Machine Tip Clearance and Vibration Measurements using a Fibre Optic Laser Doppler Position Sensor,” Meas. Sci. Technol., 17, pp. 1693-1705.
[18] Albrecht, H.-E., Borys, M., Damaschke, N., and Tropea, C., 2003, “Laser Doppler and Phase Doppler Measurement Techniques,” Springer, Berlin.
[19] Büttner, L., Czarske, J., and Knuppertz, H., 2005, “Laser Doppler Velocity Profile Sensor with Sub-Micrometer Spatial Resolution that Employs Fiber-Optics and a Diffractive Lens,” Applied Optics, 44, pp. 2274-2280.
[20] Günther, P., Dreier, F., Pfister, T., Czarske, J., Haupt, T., and Hufenbach, W., 2010, “Measurement of Radial Expansion and Tumbling Motion of a High-Speed Rotor using an Optical Sensor System”, Mechanical Systems and Signal Processing, doi:10.1016/j.ymssp.2010.08.005.

